Preprints of the 19th World Congress
The International Federation of Automatic Control
Cape Town, South Africa. August 24-29, 2014

Fault-Tolerant Control of a Unmanned Aerial Vehicle with Partial Wing Loss

Wiaan Beeton * **J.A.A. Engelbrecht** **

* *Stellenbosch University, Stellenbosch, South Africa (e-mail: wbeeton@sun.ac.za)*
** *Stellenbosch University, Stellenbosch, South Africa (e-mail: jengelbr@sun.ac.za)*

Abstract:
This paper presents the design, implementation and flight testing of a fault-tolerant flight control system for an unmanned aerial vehicle that can accommodate partial wing loss. A dynamic model for the damaged unmanned aerial vehicle (UAV) is based on an asymmetric six degrees-of-freedom equations of motion model. The effect of partial wing loss on the aerodynamic coefficients, centre of mass location and moments of inertia are calculated as a function of percentage wing loss using vortice lattice techniques and computer assisted design software respectively. The model also accounts for changes in the aileron control authority due to partial control surface loss. The equilibrium manifold of the aircraft state is determined as a function of partial wing loss by solving the nonlinear differential equations with a sequential quadratic programming algorithm. A linear parameter-varying model is then obtained by linearising the nonlinear model over the range of equilibrium states. It is found that the trim state of the aircraft changes significantly over the range of percentage wing loss, but that the stability about the trim condition does not change drastically. An acceleration-based flight control system is designed and its robustness is analysed in terms of maximum variations in gain and phase margins. A flight test is performed where 20% of the wing is jettisoned in-flight. The experimental results show that the flight control system is able to stabilise the damaged aircraft and continue with normal waypoint navigation.

Keywords: aircraft control, control system analysis, fault-tolerant systems, inherent stability, robustness

NOMENCLATURE

α	Angle of attack
$\bar{V}$	Airspeed magnitude
β	Sideslip angle
$\delta_{(\cdot)}$	Control surface $(\cdot)$ deflection
$\mathbf{v}$, $\dot{\mathbf{v}}$	Body velocity and acceleration vector
ω, $\dot{\omega}$	Angular velocity and acceleration vector
ψ, θ, ϕ	Heading, pitch and bank angles
A_w, B_w, C_w	Axial, lateral and normal specific acceleration vector components in wind axes
$C_{(\cdot)_{(\cdot\cdot)}}$	Aerodynamic coefficient relating $(\cdot)$ to $(\cdot\cdot)$
F	Force
I	Moment of inertia matrix or identity matrix
$J_{(\cdot)}$	Cost function with respect to $(\cdot)$
$k_{(\cdot)}$	Gain with respect to $(\cdot)$
L	Guidance point length
L, M, N	Moments about the x, y and z body axis
M	Moments
m	Mass
$N_{(\cdot)}$	Feed forward gain with respect to $(\cdot)$
P, Q, R	Roll, Pitch and Yaw rate
P_{W_C}	Roll rate command in the wind axis
T	Thrust
U, V, W	Velocity in x, y and z body axes
$w_{(\cdot)}$	Weighting coefficient with respect to $(\cdot)$

1. INTRODUCTION

Fault-tolerant control is one of the key enabling technologies required for the eventual integration of autonomous unmanned aircraft into commercial airspace. Certification of conventional manned aircraft requires that the pilot be able to accommodate actuator and sensor faults, as well as changes in the aircraft dynamics due to airframe damage. Certification of autonomous unmanned aircraft will require the autonomous flight control system to perform this same function. Research into fault-tolerant control can be divided into two main categories, namely accommodation of actuator and sensor faults, and accommodation of abrupt changes in the aircraft dynamics due to airframe damage. The research in this paper addresses the latter category, by designing a fault-tolerant flight control system that is able to accommodate the abrupt change in aircraft dynamics following a damage event resulting in partial wing loss.

In May 1983, an F-15D fighter aircraft of the Israeli air force experienced partial wing loss as a result of a mid-air collision with an A-4 Skyhawk during training. Even with half of the right wing missing, the pilot was still able to successfully land the aircraft, Easley (2001). Inspired by this event, several research projects were initiated to

investigate the design of automatic flight control systems that are able to perform the same feat.

In order to design a fault-tolerant control system, the effect of the aircraft damage on the flight dynamics must be modelled and understood. Shah (2008) analysed the effects of wing and tailplane damage on the aerodynamic coefficients of an aircraft. The analysis concluded that no symmetric assumptions may be made on the aircraft and biases will be introduced in the aerodynamic coefficients due to lift and drag changes as the wing's physical structure changes. Bacon and Gregory (2007) developed an asymmetric equations of motion, accounting for a shift in centre of gravity (CG) location. de Marco et al. (2007) proposed different trim scenarios. It generalised straight flight by allowing the aircraft with either a bank angle of a sideslip angle. Numerical methods were used to find the trim solutions.

The two main approaches to fault-tolerant flight control are adaptive control and robust control. In the adaptive control approach, the controller adapts to changes in the aircraft dynamics. In the robust control approach, the controller does not adapt, but is designed to provide acceptable stability and performance over the range of possible aircraft dynamics models, which include the nominal case and all damaged cases. AlSwailem (2004) developed a robust controller for a catapult launched UAV which experienced large shift in CG location. This fault is not directly related to partial wing-loss, but losing a part of a wing will result in mass loss, which will change the CG location. Boskovic et al. (2007) retrofitted a linear control architecture, designed on a nominal aircraft dynamic model, with a controller which is only active when the aircraft's dynamics leave the nominal state. This design strongly depended on the closed loop nominal system's properties. Arruda (2009) developed a control system which is resilient to asymmetric damage through dynamic inversion. It took into account the shift in CG by using the equations developed in Bacon and Gregory (2007). Chowdhary et al. (2013) implemented guidance and control architectures capable of handling actuator failures and structural damage. It focused on bounding and modifying the acceleration commands when attitude limits are exceeded. A linear controller, MRAC architecture and adaptive-loop transfer recovery method was used.

This paper presents the design, analysis, implementation and flight testing of a fault-tolerant flight control system for an unmanned aerial vehicle that can accommodate partial wing loss. The flight control design uses the acceleration-based control architecture proposed by Peddle (2008) which provides robustness to model uncertainties by encapsulating them in the innermost acceleration-level control loops. The rest of the paper is organised as follows. In section 2 the modified unmanned aerial vehicle that was used for experimental validation of the research is described, and a dynamic model for the damaged UAV is obtained. In section 3 the equilibrium manifold of the aircraft state is determined as a function of partial wing loss and an analysis is performed to determine the dominant effects on the trim settings. In section 4 the nonlinear model is linearised about the equilibrium states and the natural modes of motion are analysed over the range of partial wing loss. In section 5 the design of the fault-tolerant flight control architecture is presented, and the robustness of the flight control system is analysed in terms of the variation of the gain and phase margins over the range of partial wing loss. In section 6, the performance of the fault-tolerant control system is verified in nonlinear simulation. Section 7 presents the flight test results of a practical flight test where 20% of the main wing was jettisoned in flight.

2. DYNAMIC MODELLING WITH PARTIAL WING LOSS

2.1 Research Vehicle

A modified Phoenix Trainer 60 RC aircraft, Figure 1, with a wingspan of 2 metres was used as the demonstrator vehicle for practical verification of the research. It is equipped with a custom avionics pack designed and built at the Electronic Systems Laboratory (ESL) at Stellenbosch University. The avionics pack includes microcontrollers for control processing and estimation, an inertial measurement unit (IMU) for sensing body accelerations and angular rates, a static and dynamic pressure sensor for sensing airspeed and altitude, and a global positioning system (GPS) sensor for sensing inertial velocities and positions.

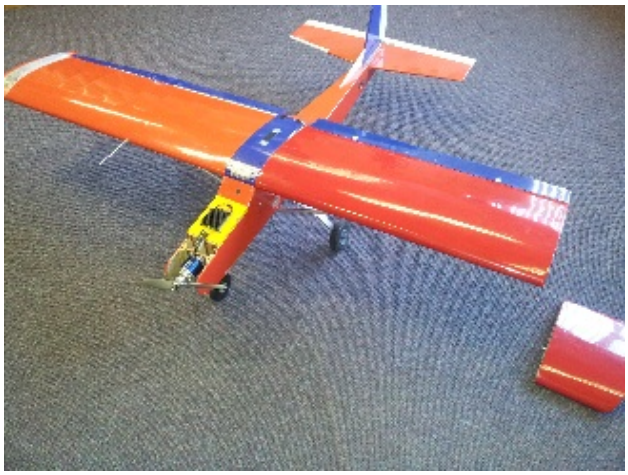

Fig. 1. Phoenix Trainer 60

Before the fault-tolerant control system can be designed, the effect of the aircraft damage on the flight dynamics must be modelled and understood. A block diagram of the model is shown in Figure 2.

The dynamic model for the damaged UAV is based on an asymmetric six degrees-of-freedom equations of motion model. The effect of partial wing loss on the aerodynamic coefficients, centre of mass location and moments of inertia are calculated as a function of percentage wing loss using vortice lattice techniques and computer assisted design software respectively. The model also accounts for changes in the aileron control authority due to partial control surface loss.

2.2 Asymmetric Equations of Motion

The equations derived in Bacon and Gregory (2007) form the basis for the mathematical model and are provided

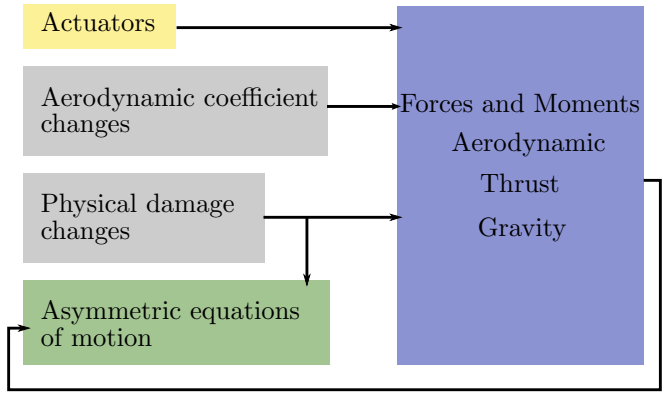

Fig. 2. Non linear model

in matrix notation in equation (1). They represent an asymmetric object, with the ability to move its CG. Δx, Δy and Δz define the CG's displacement, in this case with regards to the symmetric aircraft's CG location.

$$\begin{bmatrix} \dot{\mathbf{v}}_B \\ \dot{\omega} \end{bmatrix} = \begin{bmatrix} m\mathbf{I}_3 & -\mathbf{D}_x \\ \mathbf{D}_x & \mathbf{I} \end{bmatrix}^{-1} \left[\begin{bmatrix} \Sigma \mathbf{F} \\ \Sigma \mathbf{M}_B \end{bmatrix} - \begin{bmatrix} m\mathbf{\Omega}_x & -\mathbf{\Omega}_x \mathbf{D}_x \\ \mathbf{\Omega}_x \mathbf{D}_x & \mathbf{\Omega}_x \mathbf{I} - \mathbf{V}_x \mathbf{D}_x \end{bmatrix} \begin{bmatrix} \mathbf{v}_B \\ \omega \end{bmatrix} \right] \quad (1)$$

with

$$\mathbf{D}_x = \begin{bmatrix} 0 & -m\Delta z & m\Delta y \\ m\Delta z & 0 & -m\Delta x \\ -m\Delta y & m\Delta x & 0 \end{bmatrix}$$

$$\mathbf{\Omega}_x = \begin{bmatrix} 0 & -R & Q \\ R & 0 & -P \\ -Q & P & 0 \end{bmatrix}$$

$$\mathbf{V}_x = \begin{bmatrix} 0 & -W_B & V_B \\ W_B & 0 & -U_B \\ -V_B & U_B & 0 \end{bmatrix}$$

$$I = \begin{bmatrix} I_{xx} & -I_{xy} & -I_{xz} \\ -I_{xy} & I_{yy} & -I_{yz} \\ -I_{xz} & -I_{yz} & I_{zz} \end{bmatrix} \quad (2)$$

The equations above allow the forces and moments to be calculated around the original CG and then transferred to the new CG location. This is convenient as the aerodynamic forces and moments can easily be modelled with vortice lattice software around the original CG, thus leaving only the additional moment caused by gravity to be calculated.

2.3 Effect on Aerodynamic Coefficients

Athena Vortex Lattice (AVL) was used to model the effect of partial wing loss on the aerodynamic coefficients. A model of the full symmetric wing and tailplane was created and segmented into 10% increments of partial wing loss from the wing tip inwards. The aerodynamic coefficients were then calculated for the undamaged case, as well as for damage cases in increments of 10% partial wing loss. The aerodynamic coefficients obtained were implemented in Matlab interpolated lookup tables for simulation purposes.

Upon examining the aerodynamic coefficients, it becomes apparent that a partial loss of wing area results in a reduction in lift and drag. The asymmetric loss in lift also causes a rolling and yawing moment bias. The effectiveness of the ailerons also decreases as part of the aileron control surface is also lost. The remainder of the aerodynamic coefficients experience negligible changes. Figure 3 shows the change in the components of the aerodynamic roll coefficient as a function of percentage partial wing loss.

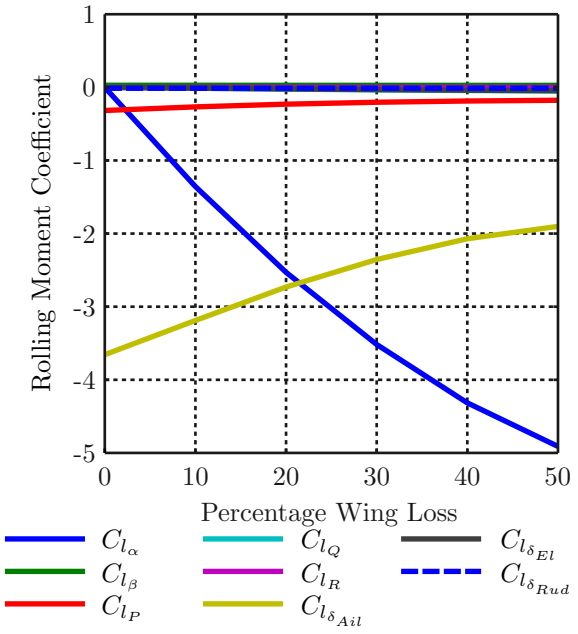

Fig. 3. Roll Coefficients

2.4 Effect on Centre of Gravity, Mass and Moment of Inertia

The effects of partial wing loss on the centre of gravity (CG), mass, and moment of inertia, was modelled using Autodesk Inventor 2011. A full model of the wing was constructed according to the measurements of the aircraft's wing, with the densities specified for every material used in the physical wing. This model was then segmented into 10% increments of partial wing loss from the wing tip, as was done for the calculating the aerodynamic coefficients. For every increment of partial wing loss, the CG, mass and moment of inertia changes were calculated and also implemented in a Matlab interpolated lookup table for simulation purposes. These values were then used in equation (1) to transform the forces and moments from the original CG to the new CG, while accounting for the new inertia properties of the aircraft.

3. ASYMMETRIC TRIM

The model derived in section 2 was used to calculate the required trim settings and resulting trim conditions of the asymmetrically damaged aircraft to be in equilibrium. A sequential quadratic programming algorithm, implemented by Jaquet (2010), was used to calculate the trim for different percentages of partial wing-loss. A cost function was constructed to allow the angle of attack α, the sideslip angle β, the bank angle ϕ and the actuator

deflection angles to be weighted relative to each other as shown in (3). Hard constraints were set that the altitude and airspeed shall remain constant, and that the body angular rates shall be zero ($P = Q = R = 0$) at equilibrium.

$$\begin{aligned} J_O &= w_\alpha \alpha^2 + (1 - w_\alpha)(w_{\beta\phi}\beta^2 + (1 - w_{\beta\phi})\phi^2) \\ J_\delta &= (w_{\delta a}\delta a^2 + w_{\delta e}\delta e^2 + w_{\delta r}\delta r^2)/w_{\delta T} \\ J_T &= (w_O J_O + w_\Delta J_\delta) / (w_O + w_\Delta) \end{aligned} \quad (3)$$

Solving for various combinations of the above cost function weighting, it was found that a minimisation of the sideslip angle β led to the equilibrium with the lowest overall cost. Figure 4 shows simulations of the uncontrolled flight of the UAV after being initialised with the calculated trim conditions and settings for 0% to 40% partial wing-loss as specified in table 1. Note that the available control authority for the ailerons, elevator, and rudder deflections are all -15 to $+15$ degrees, and the available control authority for the thrust is 0 to 42N. Notice that for any finite amount of wing loss, the equilibrium is unstable and the flight path will eventually diverge from straight and level flight if even slightly disturbed.

The challenge for the flight control system is therefore to find the valid trim settings for the specific amount of partial wing loss, and to stabilise the flight dynamics about the trim.

4. EFFECT OF PARTIAL WING LOSS ON STABILITY

Following the trim analysis, the nonlinear flight dynamics model was linearised about the trim states over the range of partial wing loss to obtain a linear parameter-varying model. A root locus analysis and a frequency response analysis was then performed to see how the relative stability of the aircraft changes as a function of partial wing loss.

4.1 Open Loop Poles

The locus of the open-loop poles as the percentage partial wing loss is varied from 0% to 40% is shown in Figure 5. The locus shows the open-loop poles for both the longitudinal and lateral modes of motion, since decoupling between longitudinal and lateral dynamics can no longer be assumed for the asymmetrically damaged aircraft. Although the longitudinal states are not significantly effected by the lateral states, the lateral states are in fact significantly effected by the longitudinal states. The locus plot shows that the locations of the open-loop poles do not change dramatically over the range of percentage partial wing loss, which indicates that the stability and transient response also do not change dramatically. The open-loop pole locations and their associated damping ratios and natural frequencies for 10% increments in partial wing loss are shown in tables 2 and 3. Since the open-loop pole locations do not change dramatically, an adaptive control strategy is not required, and a fixed-gain control strategy can be designed that is robust to the changes in the aircraft dynamics over the range of partial wing loss.

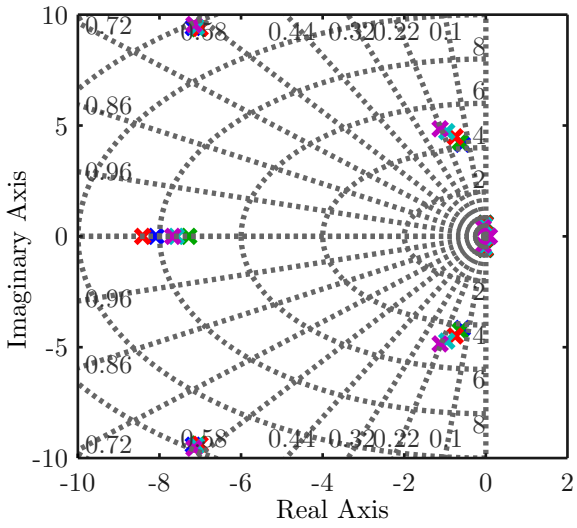

Fig. 5. Full Coupled Natural Modes

Table 2. Lateral Modes

loss	Pole ($rad.s^{-1}$)	ω_n	ζ
Dutch Roll Mode			
0%	-0.575 ± 4.15j	4.19	0.137
10%	-0.63 ± 4.26j	4.3	0.146
20%	-0.752 ± 4.49j	4.55	0.165
30%	-0.959 ± 4.72j	4.82	0.199
40%	-1.12 ± 4.85j	4.98	0.225
Roll Mode			
0%	-8.09	N/A	
10%	-7.28	N/A	
20%	-8.41	N/A	
30%	-7.59	N/A	
40%	-7.67	N/A	
Spiral Mode			
0%	0.0575	N/A	
10%	0.0616	N/A	
20%	0.0659	N/A	
30%	0.0728	N/A	
40%	0.0868	N/A	

Table 3. Longitudinal Modes

loss	Pole ($rad.s^{-1}$)	ω_n	ζ
Phugoid			
0%	-0.0119 ± 0.589j	0.589	0.0202
10%	-0.0142 ± 0.587j	0.587	0.0243
20%	-0.023 ± 0.557j	0.557	0.0413
30%	-0.0398 ± 0.496j	0.498	0.0799
40%	0.0653 ± 0.394j	0.399	0.164
Short Period			
0%	-7.17 ± 9.42j	11.8	0.606
10%	-7.04 ± 9.37j	11.7	0.601
20%	-7 ± 9.38j	11.7	0.598
30%	7.09 ± 9.44j	11.8	0.601
40%	7.16 ± 9.56j	11.9	0.599

5. CONTROL SYSTEM DESIGN

A flight control system was designed based on the acceleration-based control architecture proposed by Peddle (2008). This architecture was chosen because it provides robustness to model uncertainties by encapsulating them in the innermost acceleration-level control loops, and features integrators that are able to seek the trim settings

Table 1. SQP Calculated Trim Flight Values

	Thrust	α	β	ϕ	δ_{Ail}	δ_{El}	δ_{Rud}
0%	4.73463	6.05468	0.00000	0.00000	0.00000	-4.41453	0.00000
10%	4.70676	6.48423	-0.00000	0.00057	-2.29587	-4.66386	0.08458
20%	4.60693	6.94481	-0.00000	0.00100	-4.25040	-4.82817	0.14297
30%	4.51467	7.67429	-0.00000	0.00154	-7.22435	-5.02199	0.21400
40%	4.48637	9.11827	-0.00000	0.00250	-13.49015	-5.08720	0.33983

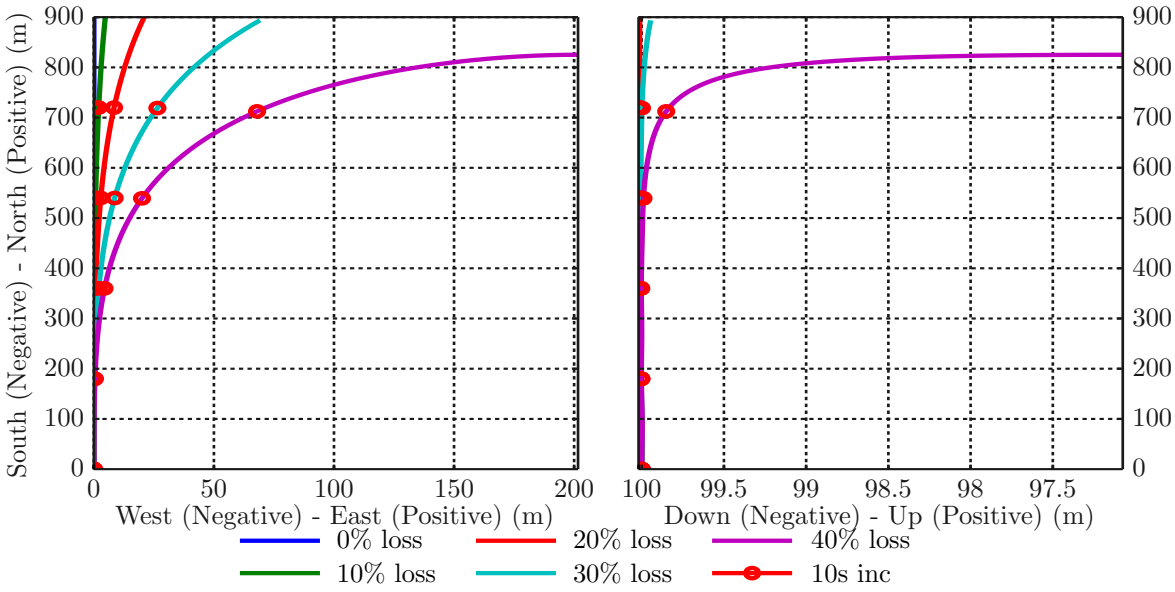

Fig. 4. SQP Trim Flight with Wing-loss

for equilibrium. The block diagram of the flight control system is shown in Figure 6. The estimator shown in the figure is a kinematic estimator, estimating the UAV's position, velocity, angular rates and attitude from sensor measurements.

The airspeed controller is an augmented PI controller, with the control law as stated in equation (4) and described in de Hart (2010). T' serves as a feedforward term to negate gravity.

$$T_c = -k_v \bar{V} - k_e E_v + T' \quad \text{with} \quad \dot{E}_v = \bar{V} - \bar{V}_{ref} \tag{4}$$

The Dutch roll damper follows the classical design and is implemented as a washout filter in the feedback loop from yaw rate measurement to rudder deflection.

The Normal Specific Acceleration controller is a PI controller that implements the control law in equation (5) and described in Peddle (2008).

$$\delta_{El} = -k_Q Q - k_C C_w - k_E E_C + \delta'_{El} \quad \text{with} \quad \dot{E}_C = C_W - C_{W_{ref}} \tag{5}$$

The roll rate and bank angle controllers are PI and P controllers respectively that implement the control laws in equations (6) and described in Peddle (2008).

$$\delta_{Ail} = -k_P P - k_E E_P + N_P P_R \quad \text{where} \quad \dot{E}_P = P - P_R$$

$$\text{and} \quad P_R = P_{W_C} + k_\phi \phi \tag{6}$$

The climb rate and altitude controllers are both implemented as proportional controllers, with the climb rate controller commanding a vertical acceleration. The cross track controller implements the nonlinear guidance law shown in equation (7) and described in Park et al. (2004) to command a lateral acceleration. The vertical and lateral acceleration commands are combined to obtain a specific normal acceleration command and a bank angle command.

$$B_{cmd} = \frac{2}{|L|^2} \left(\bar{V} \times L \right) \times \bar{V} \tag{7}$$

The variation of the gain and phase margins of all controllers were analysed over the range of 0% to 40% partial wing loss. The worst stability margins over all the controllers and over the entire range of percentage partial wing loss are 5.6dB gain and 46.8° phase margin. This indicates that the fixed-gain acceleration-based control architecture is sufficienty robust to the variation in the aircraft dynamics over the range of expected partial wing loss percentages.

6. PARTIAL WING-LOSS EVENT SIMULATION

Nonlinear simulations were performed to verify the flight control system's ability to accommodate a partial wing loss event. The simulation was initialised with a healthy undamaged aircraft flying straight and level under automatic flight control. At a certain point in the simulation a partial wing loss event was introduced, and the response

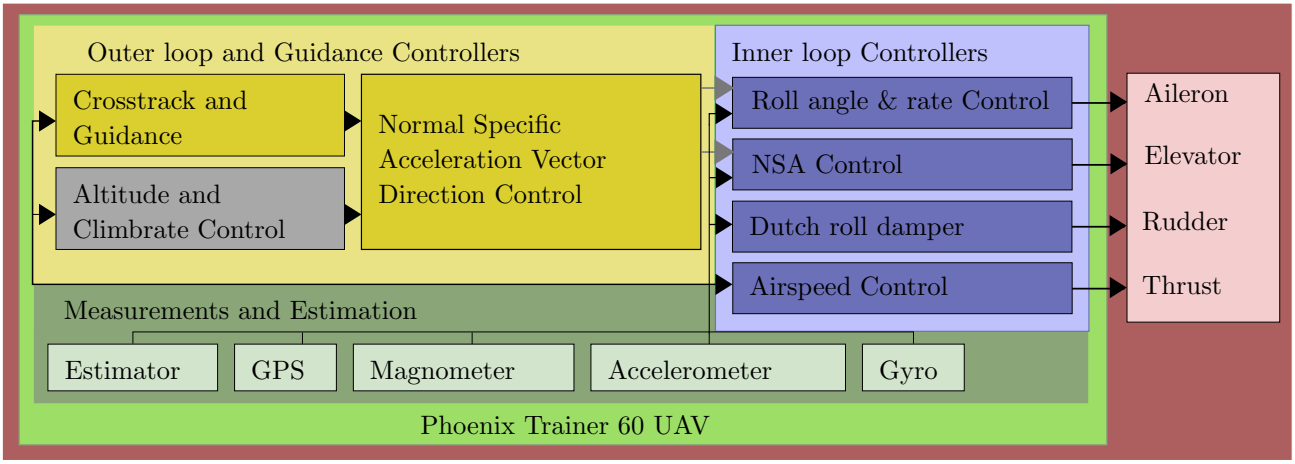

Fig. 6. Control System

of the flight control system to the event was observed. The simulated time histories of the cross track error, altitude, and aileron deflections before, during and after the partial wing loss event are shown in Figures 7 to 9 for 0% to 30% partial wing loss percentages.

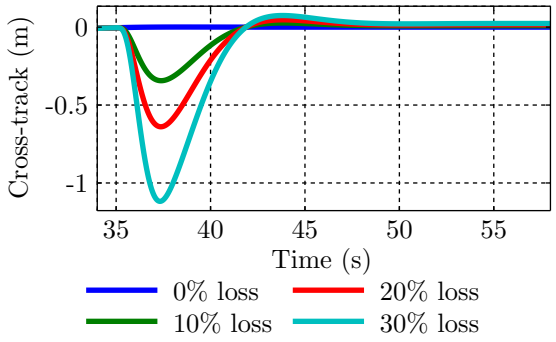

Fig. 7. Simulation - Loss recovery - Cross-track

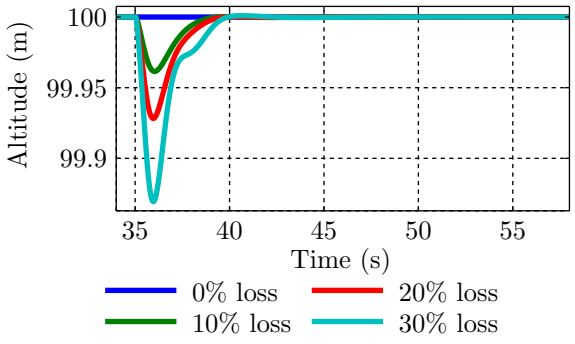

Fig. 8. Simulation - Loss recovery - Altitude

The time histories exhibit a transient after the partial wing loss event, but the flight control system quickly finds the new valid trim settings, and the aircraft settles to the new trim condition for the damaged asymmetric aircraft. The steady-state actuator settings agree well with the trim actuator settings calculated in section 3.

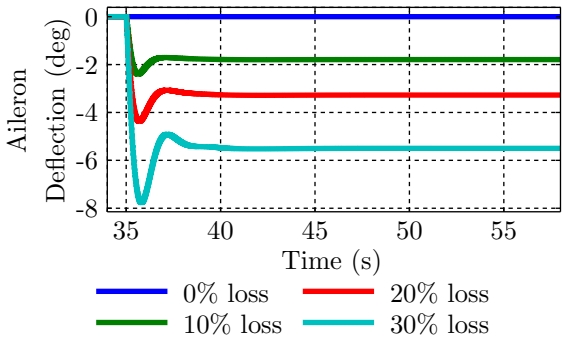

Fig. 9. Simulation - Loss recovery - Ailerons

7. FLIGHT TEST RESULTS

Flight tests were performed with the modified Trainer 60 UAV to practically verify the flight control system's ability to accommodate a partial wing loss. A release mechanism was designed and built to enable 20% of the aircraft's left wing to be jettisoned during flight. The aircraft was flown under automatic control and commanded to navigate a sequence of waypoints. During one of the waypoint legs, the detachable part of the left wing was jettisoned, and the response of the flight control system was observed.

The measured time histories of the circuit and aileron deflections before, during and after the partial wing loss event are shown in Figures 10 and 11. The flight test results show that the ailerons quickly find the new valid trim settings, that the aircraft remains stable, and continues to complete its circuit. The aileron's new trim deflection compares well with the simulated trim deflection after a bias is removed due to misalignment of the IMU.

8. CONCLUSION

A flight dynamics model for a UAV with partial wing loss was constructed by modelling the effects of partial wing loss on the aerodynamic coefficients, mass, moment of inertia, and centre of gravity of the aircraft, and integrating them into an existing asymmetric six degrees-of-freedom equations of motion model. The trim conditions and linearised dynamics about the trim conditions were obtained and analysed as a function of percentage partial

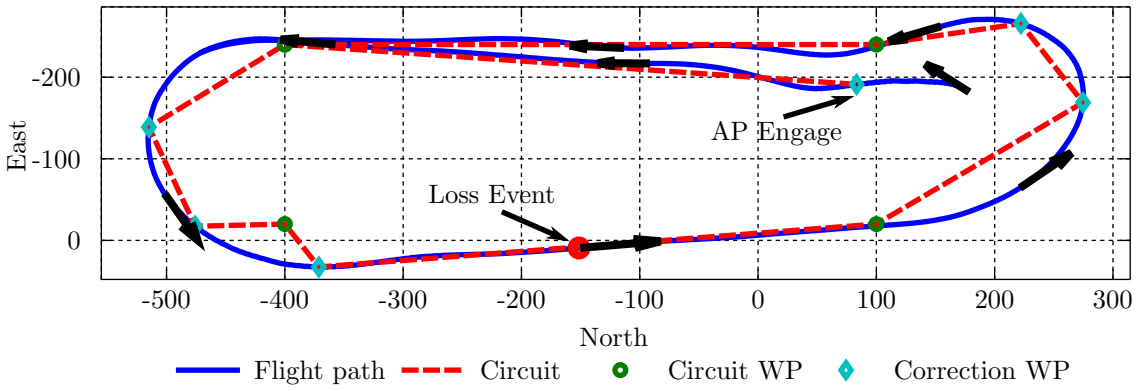

Fig. 11. Flight - Loss recovery - Circuit

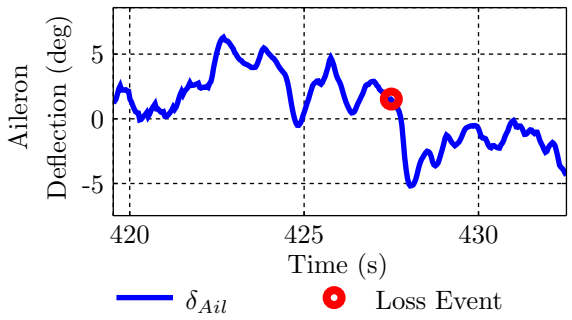

Fig. 10. Flight - Loss recovery - δ_{Ail}

wing loss. The analysis indicated that the required trim settings change dramatically after a partial wing loss, but that the dynamics linearised around the equilibrium does not change significantly. A fault-tolerant flight control system was designed that uses integrators in the inner-most acceleration loops to find the new trim actuator settings, and uses fixed-gain feedback controllers to stabilise the flight dynamics about the trim condition. The variations in gain margins and phase margins were analysed as a function of percentage partial wing loss, and it was shown that all controllers are sufficiently robust. The fault-tolerant flight control system's ability to accommodate partial wing loss events was verified with nonlinear simulations from 0% to 30% wing loss, and was successfully demonstrated with practical flight tests where 20% of the left wing was jettisoned during flight.

REFERENCES

AlSwailem, S. (2004). *Application of Robust Control in Unmanned Vehicle Flight Control System Design.* Ph.D. thesis, Cranfield University.

Arruda, M. (2009). *Dynamic Inverse Resiliant Control For Damaged Asymmetric Aircraft: Modeling And Simulation.* Master's thesis, Wichita State University.

Bacon, B. and Gregory, I. (2007). General equations of motion for a damaged asymmetric aircraft.

Boskovic, J., Prasanth, R., and Mehra, R. (2007). Retrofit fault-tolerant flight control design under control effector damage.

Chowdhary, G., Johnson, E., Chandramohan, R., Kimbrell, M., and Calise, A. (2013). Guidance and control of airplanes under actuator failures and severe structural damage.

de Hart, R. (2010). *Advanced Take-off and Flight Control Algorithms for Fixed Wing Unmanned Aerial Vehicles.* Master's thesis, Stellenbosch University.

de Marco, A., Claudio, V., and Duke, E. (2007). A general solution to the aircraft trim problem. *AIAA Modeling and Simulation Technologies Conference and Exhibit.*

Easley, J. (2001). F-15. URL `http://www.uss-bennington.org/phz-nowing-f15.html`.

Jaquet, C. (2010). *Control Surfaces in Confined Spaces: The optimisation of trailing edge tabs to reduce control surface hinge moments.* Master's thesis, Stellenbosch University.

Park, S., Deyst, J., and How, J. (2004). A new nonlinear guidance logic for trajectory tracking.

Peddle, I. (2008). *Acceleration Based Manoeuvre Flight Control System for Unmanned Aerial Vehicles.* Ph.D. thesis, University of Stellenbosch.

Shah, G. (2008). Aerodynamic effects and modelling of damage to transport aircraft. In *AIAA Atmospheric Flight Mechanics Conference and Exhibit.* American Institute of Aeronautics and Astronautics.